

## Density-Dependent Reorientation and Rehybridization of Chemisorbed Conjugated Molecules for Controlling Interface Electronic Structure

B. Bröker,<sup>1</sup> O. T. Hofmann,<sup>2</sup> G. M. Rangger,<sup>2</sup> P. Frank,<sup>2</sup> R.-P. Blum,<sup>1</sup> R. Rieger,<sup>3</sup> L. Venema,<sup>4</sup> A. Vollmer,<sup>5</sup> K. Müllen,<sup>3</sup> J. P. Rabe,<sup>1</sup> A. Winkler,<sup>2</sup> P. Rudolf,<sup>4</sup> E. Zojer,<sup>2</sup> and N. Koch<sup>1,\*</sup>

<sup>1</sup>*Institut für Physik, Humboldt-Universität zu Berlin, Newtonstrasse 15, D-12489 Berlin, Germany*

<sup>2</sup>*Institute of Solid State Physics, Graz University of Technology, Petersgasse 16, A-8010 Graz, Austria*

<sup>3</sup>*Max Planck Institut für Polymerforschung, Ackermannweg 10, D-55128 Mainz, Germany*

<sup>4</sup>*Zernike Institute for Advanced Materials, University of Groningen, Nijenborgh 4, 9747 AG Groningen, The Netherlands*

<sup>5</sup>*Helmholtz-Zentrum Berlin für Materialien und Energie GmbH, BESSY II, D-12489 Berlin, Germany*

(Received 21 January 2010; published 18 June 2010)

The adsorption of the molecular acceptor hexaazatriphenylene-hexacarbonitrile on Ag(111) was investigated as function of layer density. We find that the orientation of the first molecular layer changes from a face-on to an edge-on conformation depending on layer density, facilitated through specific interactions of the peripheral molecular cyano groups with the metal. This is accompanied by a rehybridization of molecular and metal electronic states, which significantly modifies the interface and surface electronic properties, as rationalized by theoretical modeling.

DOI: 10.1103/PhysRevLett.104.246805

PACS numbers: 73.20.-r, 68.55.am, 68.35.bm, 73.30.+y

Understanding the fundamental mechanisms that determine the properties of interfaces between metals and conjugated organic materials is a key prerequisite for advancing the fields of *organic* and *molecular electronics*, where the (opto-)electronic function of devices depends critically on, e.g., charge density distribution [1,2], energy level hybridization and interface state formation [1,3,4], molecular conformation changes [3–6], and energy level alignment [5,7–9]. Additionally, it has been shown recently that the ionization energy of ordered molecular layers depends critically on the surface orientation of molecules, and that the energy levels at interfaces can be manipulated *via* molecular orientation [10]. However, it is commonly accepted that the orientation of a conjugated molecular monolayer with respect to a metal electrode surface is set for a particular material pair, only depending on the relative strength of metal-molecule and intermolecular interactions. If substrate-molecule interactions prevail, as for clean metal surfaces, at least the first molecular layer is found to be face-on [11–13]. Only multilayers are known to eventually adopt a different orientation [13–15] because the strong interaction with the metal is already screened by the monolayer. Here, we demonstrate the molecular density-dependent reorientation of an entire stable face-on monolayer to a stable edge-on conformation, which is achieved through balancing the surface energy in the two orientations by enabling strong hybridization of molecular and metal electronic states in *both* orientations through functional terminal groups. Particularly, the chemisorbed molecular state in the edge-on monolayer exhibits extraordinary electronic properties with a potential for huge application relevance, which is not the case for the face-on orientation.

Ultraviolet photoelectron spectroscopy (UPS) spectra were taken at the end station SurICat at BESSY II

(Berlin). Kelvin-probe (KP) and thermal desorption spectroscopy (TDS) was done at the Graz University of Technology (Graz), and reflection absorption infrared spectroscopy (RAIRS) at the Zernike Institute for Advanced Materials (Groningen). All sample preparation steps and measurements were performed at room temperature and in ultrahigh vacuum. Metal single crystals were cleaned by repeated cycles of heating and sputtering and molecules were sublimed from pinhole sources. Further details can be found in the supporting information [16], where also details on the density-functional theory (DFT) calculations employed in this study are reported.

Hexaazatriphenylene-hexacarbonitrile (HATCN, chemical structure shown in the inset of Fig. 2) is a strong electron acceptor without an intrinsic dipole moment, which was here chemisorbed on Ag(111). The Ag(111) surface work function ( $\Phi$ ) changes due to HATCN deposition as shown in Fig. 1, determined independently by UPS and KP measurements. A pronounced deviation from the expected dependence of sample  $\Phi$  on acceptor coverage ( $\theta$ ) is observed, as three regimes instead of two occur: (i) for low  $\theta$ ,  $\Phi$  is essentially constant (from 0 Å to  $\sim 2.5$  Å [17], highlighted in red (dark gray) in Fig. 1), (ii) followed by a strong and almost linear  $\Phi$  increase by  $\sim 1$  eV (from  $\sim 2.5$  Å to  $\sim 8$  Å, highlighted in black); (iii) finally a saturation of  $\Phi$  is reached [beyond  $\sim 8$  Å, highlighted green (light gray)]. The value of  $\Phi$  changes from 4.4 eV [pristine Ag(111)] to 5.4 eV [ $26$  Å HATCN/Ag(111)]. Commonly, the deposition of acceptors on metal surfaces involving net metal-to-acceptor electron transfer leads to the observation of regime (ii) from the very beginning, followed by regime (iii) [18]. Such a “delayed” increase of  $\Phi$ , i.e., the additional appearance of regime (i), has not been reported before and cannot be rationalized on the basis of the Helmholtz-equation (or the Topping model

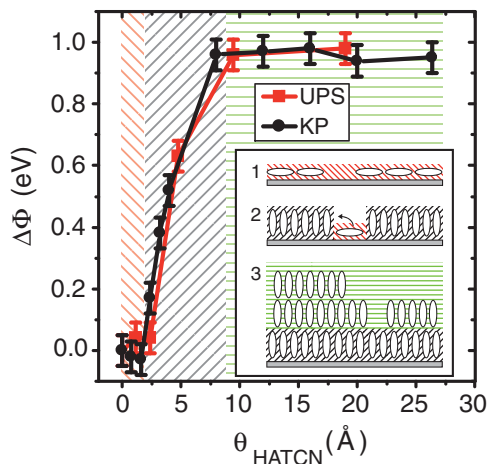


FIG. 1 (color online). Work function change  $\Delta\Phi$  relative to pristine Ag(111) as a function of nominal HATCN thickness  $\theta$ , obtained by UPS (red squares) and KP (black dots). The inset shows the proposed density-dependent orientation of HATCN on Ag(111). The color coding of the background shading represents the three different regimes referred to throughout the text: red (dark gray) = regime (i), black = regime (ii), and green (light gray) = regime (iii).

including dipole-dipole depolarization effects [19]) when assuming any of the known growth models of conjugated molecules on metal surfaces. As regime (ii) sets in after completion of a face-on nominal monolayer of HATCN [20], a considerable electron transfer from the metal also into HATCN multilayers would have to be invoked, which is inconsistent with the present understanding of organic-metal interface energetics [21]. The situation is further complicated by the fact that several possible orientations of molecules on top of the first face-on layer may occur. Hence, without exact knowledge of the orientation of HATCN molecules on Ag(111) and its evolution with  $\theta$ , an explanation for  $\Phi$  throughout regimes (i)–(iii) is impossible.

The quantitative analysis of TDS experiments for various initial HATCN  $\theta$  on Ag(111) is shown in Fig. 2, where the desorption of intact molecules ( $m = 384$  g/mol) and HATCN fragments is plotted ( $C_2N_2$ ,  $m = 52$  g/mol); no other HATCN fragments were observed. One possible fragment of mass 52 is highlighted by the red rectangle in the inset of Fig. 2. Alternatively, only the terminal CN groups might desorb as radicals and react to form  $C_2N_2$  [22]. Consistent with the evolution of  $\Phi$ , Fig. 2 also displays three regimes: For  $\theta$  up to  $\sim 2.5$  Å no desorption of any HATCN fragments is observed throughout the entire accessible temperature range (up to 900 K). This is indicative of a HATCN layer strongly bonded to the Ag(111) surface. Between 2.5 and 8 Å, only desorbing  $C_2N_2$  fragments are detected and virtually none of the molecules desorb intact. This shows that also in regime (ii) HATCN is strongly bonded to the metal, which would not be the case

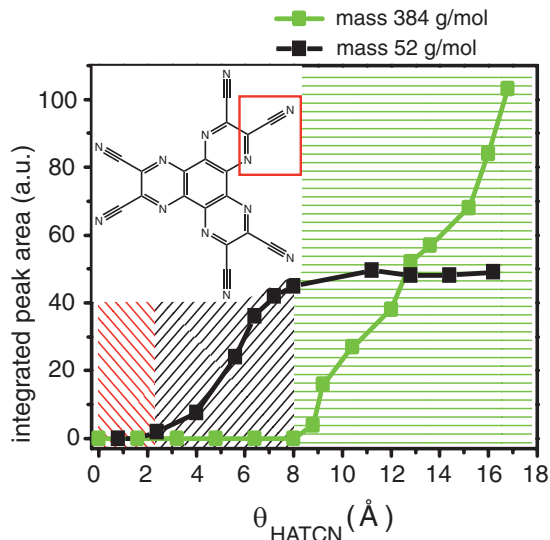


FIG. 2 (color online). TD spectra of mass 384 g/mol (HATCN) and mass 52 g/mol (HATCN fragment  $C_2N_2$ , see red rectangle in inset) for different  $\theta$  on Ag(111). Data points were obtained by integrating the peak areas in the original TD spectra. The inset shows the chemical structure of HATCN.

if they were part of a second layer. Instead, all molecules for  $\theta$  up to 8 Å must be in direct contact with the Ag(111) substrate, and thus two different types of chemisorbed HATCN states (one for  $\theta$  below 2.5 Å and one for thicknesses between 2.5 Å and 8 Å) exist. Beyond 8 Å an abrupt transition occurs: the thermal desorption (TD) signal intensity associated with fragments saturates and desorption of intact molecules starts. The latter signal increases roughly linearly with  $\theta$  and is thus associated with relatively weakly bonded multilayers. The constant  $C_2N_2$  signal implies that a HATCN layer equivalent to that of an initial  $\theta$  of 8 Å exists below the multilayers.

The orientation and relative abundance of the two chemisorbed HATCN states in the first layer were further investigated by RAIRS. Here, the surface selection rules state that only those modes are observable, for which the dipole moment changes perpendicular to the surface [23]. HATCN in KBr serves as a reference for neutral molecules, and the region of the  $C \equiv N$  stretching vibrations is shown in Fig. 3, with a strong mode at  $2241$   $cm^{-1}$  and a weaker one at  $2251$   $cm^{-1}$ . The RAIR spectra recorded *in situ* for sequential deposition of HATCN on Ag(111) are also shown in Fig. 3. Three characteristic peaks are observed, whose intensity changes as function of  $\theta$ . From the very beginning a broad mode at  $2185$   $cm^{-1}$  is seen (mode I), exhibiting a Fano-type line shape (for details see [16]), which is reminiscent of dynamical charge transfer between substrate and molecule [24]. The strong shift of this  $C \equiv N$  stretching mode to lower energy compared to neutral HATCN indicates that the adsorbed molecule is negatively charged [25]. Mode I achieves its maximum intensity at  $\theta \sim 2.7$  Å, where another mode at  $2229$   $cm^{-1}$  (mode II)

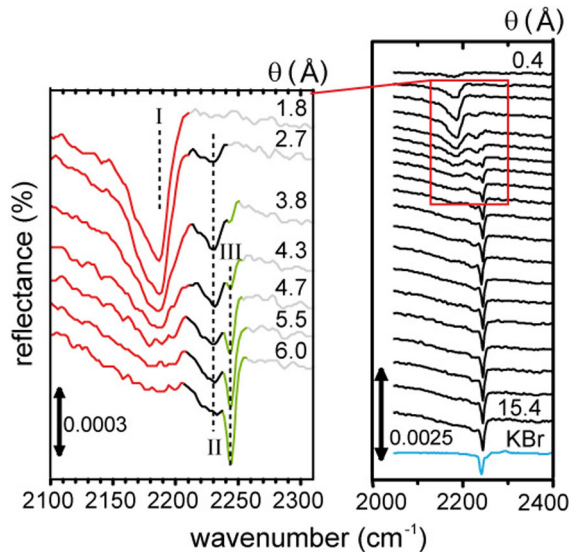


FIG. 3 (color online). Right: RAIR spectra recorded during HATCN deposition on Ag(111) for the region of the  $C \equiv N$  stretch mode. Left: Zoom of right part (denoted by the red rectangle in the right panel) for  $\theta$  up to 6 Å. The color coding of the different spectral regions refers to the three regimes (i)–(iii) used in the text.

appears in the spectra. For higher  $\theta$ , the intensity of mode I decreases, while the intensity of mode II saturates and can still be well resolved at  $\theta = 15.4$  Å. Starting at  $\theta = 3.8$  Å, a rather sharp mode at  $2243 \text{ cm}^{-1}$  (mode III) rises, which is the only one that continuously keeps increasing for higher  $\theta$ . Mode I is attributed to face-on HATCN in direct contact with the Ag(111) surface, consistent with [20]. In this conformation the mode is IR active because of dynamical charge transfer between molecule and surface and a nonplanar conformation of the molecule (*vide infra*). The most striking observation is that this mode completely vanishes for  $\theta \sim 8$  Å, which is another clear indication that the initial face-on HATCN chemisorbed state disappears. The intensity decrease of mode I begins at  $\sim 2.5$  Å, similar to the onset of the desorption of HATCN fragments in the TDS experiments. Mode II is associated with a HATCN state in which the molecules stand edge-on (possibly somewhat inclined) on the surface. In that case, two of the  $C \equiv N$  groups are bonded to the surface, while the other four only very weakly—if at all—are involved in the molecular interaction with the surface. The smaller energy shift of mode II relative to the mode of neutral HATCN in KBr compared to mode I results from the bond weakening due to charge transfer to the  $C \equiv N$  groups, which is partially compensated by C and N atoms now oscillating “between” the Ag surface atoms and the rest of the molecule. As mode III is very sharp and its position is close to modes of HATCN in KBr it is attributed to originate from multilayer HATCN, possibly superimposed by the vibrations of the nonbonded  $C \equiv N$  groups in the now edge-on oriented monolayer.

The (re-)orientation of HATCN in the first few layers is schematically summarized in the inset of Fig. 1, where three regimes can be distinguished, as was already the case in the initial observation of the  $\Phi$  change in Fig. 1. Therefore, a direct link between orientation of the molecules and  $\Phi$  can be established: In the initial stage of film growth (from 0 Å to  $\sim 2.5$  Å), the molecules are lying face-on and  $\Phi$  remains constant. With further deposition, the chemisorbed face-on HATCN molecules reorient and are incorporated into a monolayer, where the molecules are aligned edge-on in a different chemisorption state. This particular rearrangement leads to the large  $\Phi$  increase until saturation is reached at the end of regime (ii). We emphasize that the reorientation cannot be induced by thermal annealing, and that the face-on chemisorbed layer is stable for several days as long as no further HATCN is deposited. Experiments for HATCN deposited on Cu(111) substrates yielded fully analogous results in terms of reorientation and work function change regimes ( $\Delta\Phi$ ).

To understand the mechanisms for the behavior of  $\Phi$ , the face-on and edge-on HATCN layers on Ag(111) were modeled by DFT. For the face-on conformation of regime (i) (assuming the structure from [20]) we find that the charge transfer (CT) significantly outweighs Pauli repulsion, giving a  $\Phi$  change of  $\Delta\Phi_{\text{CT}} = +0.7 \text{ eV}$ . However, since the  $C \equiv N$  groups at the periphery of HATCN bend down towards the surface (Fig. 4(a) and Ref. [20]), a dipole in the opposite direction is created, yielding a molecular conformation related  $\Phi$  change  $\Delta\Phi_{\text{Mol}} = -0.5 \text{ eV}$ . As a net result a small  $\Phi$  increase of  $+0.2 \text{ eV}$  is obtained by DFT.

For the edge-on conformation of HATCN in regime (ii), no experimental evidence for an ordered molecular layer could be provided yet, which points to a disordered layer or a very complex surface unit cell (as already found for bulk HATCN *vide supra*). Thus a  $2 \times 3\sqrt{3}$  unit cell containing a single upright standing molecule was chosen for the calculations (for details see [16]). In this conformation geometric distortions of the molecule are small and  $\Delta\Phi_{\text{Mol}}$  falls below  $+0.1 \text{ eV}$ . The mechanism of CT between metal and molecule is altered fundamentally by the reorientation.

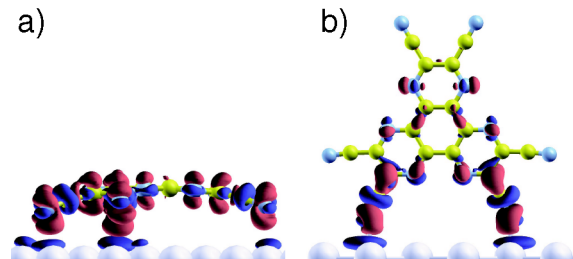


FIG. 4 (color online). Charge rearrangements upon adsorption in the face-on (a) and the edge-on (b) HATCN conformation as inferred from DFT. Red (medium gray) indicates increased electron density, blue (dark gray) electron density depletion.

Figures 4(a) and 4(b) show the charge rearrangements upon adsorption of HATCN in the two orientations. For the face-on conformation in regime (i) the whole molecule is involved in the interaction with the substrate, including  $\sigma$  electrons of the  $C \equiv N$  groups as well as the entire  $\pi$  system. For the edge-on conformation, the CT becomes more localized on the “docking groups” (here:  $C \equiv N$ ), similar to typical self-assembled monolayers [26]. The charge redistribution on the molecular backbone only plays a minor role. Yet the charge rearrangements occur over a larger distance than in the face-on conformation. In conjunction with the increased packing density and the vanishing  $\Delta\Phi_{\text{Mol}}$ , this results in an increase of  $\Phi$  by +2.4 eV. The results for both regimes (i) and (ii) are at least in qualitative agreement with the experimental observations, as they show that the  $\Phi$  change of the face-on monolayers is negligible compared to that induced by the edge-on layer. A better (i.e., quantitative) correlation between theory and experiment cannot be expected, particularly considering the unknown structure of the edge-on layer.

The microscopic origin of the density-dependent molecular reorientation must be sought in a subtle interplay of various effects. The  $\sigma$ -bonding strength between the  $C \equiv N$  groups and the metal through the N lone pair can be expected to be larger for edge-on molecules; at low  $\theta$ , it is, however, still favorable for HATCN to adsorb in a face-on geometry bringing all six  $C \equiv N$  groups into contact with the metal, and maximizing the interactions with the substrate while at the same time minimizing the metal surface energy. Once the number of molecules is larger than needed to close the face-on layer, the total number of  $C \equiv N$  groups in contact with the metal and their respective bonding strength is increased when at least part of the molecules change to edge-on. Thus, the presence of the functional groups at the periphery of HATCN facilitates the reorientation of the layer, while in their absence the second layer would just grow in a different orientation on the unchanged face-on monolayer. In our specific example, the structural change of the molecular monolayer was accompanied by a significant change in surface functionality; i.e.,  $\Phi$  for the edge-on layer was 1 eV higher than for the face-on layer or pristine Ag. In comparison, a monolayer of the widely used strong acceptor tetrafluoro-tetracyanoquinodimethane could increase  $\Phi$  of Ag surfaces by only 0.6 eV [27]. This renders the high  $\Phi$  surface an interesting candidate as hole injecting electrode in electronic devices, as the absolute  $\Phi$  value of 5.4 eV parallels that of atomically clean Au, however, the electron “pushback” effect, which is detrimental for achieving low hole injection barriers on clean metal surfaces [2,7] is expected to be minimized by the surface termination with the molecule. Also, it might be interesting to evaluate whether interface dipoles reported for other organic-metal interfaces involve in part a contribution from a multilayer-

induced reorientation of the buried monolayer in direct contact with the metal.

Financial support by the EC (NMP-3-CT-2006-033197), the Emmy-Noether-Program (DFG, 31408814), the Austrian Science Fund (P19197), the Dutch Foundation for Fundamental Research on Matter (FOM), and by the Breedtestrategie program of the University of Groningen is gratefully acknowledged.

---

\*nkoch@physik.hu-berlin.de

- [1] H. Vázquez *et al.*, *Europhys. Lett.* **65**, 802 (2004).
- [2] P. S. Bagus, K. Hermann, and C. Wöll, *J. Chem. Phys.* **123**, 184109 (2005).
- [3] A. Hauschild *et al.*, *Phys. Rev. Lett.* **94**, 036106 (2005).
- [4] L. Romaner *et al.*, *Phys. Rev. Lett.* **99**, 256801 (2007).
- [5] N. Koch *et al.*, *J. Am. Chem. Soc.* **130**, 7300 (2008).
- [6] C. Stadler, S. Hansen, I. Kröger, C. Kumpf, and E. Umbach, *Nature Phys.* **5**, 153 (2009).
- [7] H. Ishii, K. Sugiyama, E. Ito, and K. Seki, *Adv. Mater.* **11**, 605 (1999).
- [8] M. A. Baldo and S. R. Forrest, *Phys. Rev. B* **64**, 085201 (2001).
- [9] Q. Huang *et al.*, *J. Am. Chem. Soc.* **127**, 10227 (2005).
- [10] S. Duhm *et al.*, *Nature Mater.* **7**, 326 (2008).
- [11] Y. Zou *et al.*, *Surf. Sci.* **600**, 1240 (2006).
- [12] F. Schreiber, *Phys. Status Solidi A* **201**, 1037 (2004).
- [13] G. Witte and C. Wöll, *Phys. Status Solidi A* **205**, 497 (2008).
- [14] S. D. Ha, B. R. Kaafarani, S. Barlow, S. R. Marder, and A. Kahn, *J. Phys. Chem. C* **111**, 10493 (2007).
- [15] S. A. Burke, J. M. Topple, and P. Grutter, *J. Phys. Condens. Matter* **21**, 423101 (2009).
- [16] See supplementary material at <http://link.aps.org/supplemental/10.1103/PhysRevLett.104.246805> for details of the experimental and theoretical methodology and additional RAIRS data.
- [17] The coverage values refer to the nominal mass thickness as read from the quartz crystal microbalance. 2.5 Å correspond to ca. one monolayer of face-on lying HATCN molecules.
- [18] N. Koch, S. Duhm, J. P. Rabe, A. Vollmer, and R. L. Johnson, *Phys. Rev. Lett.* **95**, 237601 (2005).
- [19] A. Natan, L. Kronik, H. Haick, and R. Tung, *Adv. Mater.* **19**, 4103 (2007).
- [20] H. Glowatzki *et al.*, *Nano Lett.* **8**, 3825 (2008).
- [21] R. Forker, C. Golnik, G. Pizzi, T. Dienel, and T. Fritz, *Org. Electron.* **10**, 1448 (2009).
- [22] M. Bridge, R. Marbrow, and R. Lambert, *Surf. Sci.* **57**, 415 (1976).
- [23] F. M. Hoffmann, *Surf. Sci. Rep.* **3**, 107 (1983).
- [24] D. C. Langreth, *Phys. Rev. Lett.* **54**, 126 (1985).
- [25] P. S. Szalay, J. R. Galán-Mascarós, R. Clérac, and K. R. Dunbar, *Synth. Met.* **122**, 535 (2001).
- [26] G. Heimel, L. Romaner, J. Bredas, and E. Zojer, *Phys. Rev. Lett.* **96**, 196806 (2006).
- [27] G. M. Ränger *et al.*, *Phys. Rev. B* **79**, 165306 (2009).